Fluctuation-induced forces governed by the dielectric properties of water, a contribution to the hydrophobic interaction

H. Berthoumieux[1,2] and A.C. Maggs[3]
[1)] *Sorbonne Universités, UPMC Univ Paris 06, UMR 7600, LPTMC, F-75005, Paris, France*
[2)] *CNRS, UMR 7600, LPTMC, F-75005, Paris, France*
[3)] *Laboratoire PCT, Gulliver CNRS-ESPCI UMR 7083, 10 rue Vauquelin,75231 Paris Cedex 05, France*

The hydrophobic interaction between objects immersed in water is typically attractive and adds to the well-known van der Waals interaction. The former supposedly dominates the latter on nanometric distances and could be of major importance in the assembly of biologic objects. Here we show that the fluctuation-induced attraction between two objects immersed in a correlated dielectric medium which models water is the sum of a van der Waals term and a short-range contribution that can be identified as part of the hydrophobic interaction. In this framework, we calculate analytically the fluid correlation function and the fluctuation-induced force between small and extended inclusions embedded in water and we characterize the hydrophobic terms.

I. INTRODUCTION

The earliest direct force measurement between hydrophobic surfaces was reported in 1982 by Parshley and Israelachvili[1]. They showed that the observed interactions deviate from the expected sum of electrical double layer repulsion and van der Waals long-range attraction and highlighted the importance of a short-range hydrophobic attraction. This interaction was reported as an exponentially decaying force with a decay length of about 1 nm measurable out to a range of 10 nm. In the years following this initial study, experimental observations have found wildly varying ranges and magnitudes of hydrophobic interactions, including reports of interaction extending over a distance of several micrometers[2]. This variety of results is now attributed to the difficulty of preparation of hydrophobic surfaces. Plates were made hydrophobic using coating surfactants that rearrange in charged patches when the surfaces are immersed in liquid. The interaction between these patches generates long-range forces[3,4]. Moreover, another long-range attraction (> 300 nm) was shown to arise from bridging nano-bubbles that nucleate on the surfaces if the medium is not totally degased. Recently, the hydrophobic interaction was measured using systems that were designed to avoid these long-range biases[5,6]. These experiments report a short-range attraction with an exponential decay length which value varies from 0.3 to 1 nm depending on experimental systems.

Objects immersed in water affect the orientation and the dynamics of the fluid molecules located in the first hydration layers[7], more distant layers keep bulk properties. In the frame of a continuous field description of water, this short-range effect can be modeled by constraints imposed on the field at object boundaries. Then, the free energy of the system depends on the distance between the inclusions generating a fluctuation-induced interaction mediated by the medium[8,9]. This is known as the Casimir-like interaction and it has been extensively studied for correlated media such as critical fluids[8,9], liquid crystals[10] or membranes[11]. Within this framework, hydrophobicity was modeled as the perturbation of the density fluctuation generated by objects embedded in the fluid[12]. Bulk density correlations vanish beyond 1 nm[13]. Large hydrophobic objects induce a disruption of water hydrogen-bond network which generates a soft fluctuating water interface[28] and a partial drying of the object surface. This creates rare large density fluctuation events that can lead to the association of two large bodies separated by a nanometric distance.[12,14,15]. Density fluctuations are thus a key ingredient of the hydrophobic interaction. However a description based on the density cannot give rise to the long range van der Waals attraction that has an electrostatic origin.

Water as a fluctuating, classical fluid generates a long-range Keesom (dipole-dipole) interaction that decays with distance as $1/r^6$. On molecular scales, the integrity of the hydrogen-bond network puts significant constraints on possible orientational correlations of the water dipoles. These constraints are due to the high energy cost ($\approx 10\ k_bT$ per bond) necessary to disrupt these non-covalent bonds. Orientational correlations have been studied in ice vertex models. Water is described as a lattice in which vertices and edges represent oxygen atoms and O-H bounds respectively[16]. The network in which each oxygen is involved in two hydrogen bonds is a critical system. Criticality is avoided by the possibility of creating Bjerrum defects. The orientational correlations are an important source of entropy in water, and thus could be a contribution to the interactions between surfaces or inclusions[17,18].

Water is thus a dipolar fluid with strong intermolecular interactions and correlations and as a consequence it presents a peculiar non-local dielectric response. Computer simulations and experimental data based on neutron diffraction experiments furnish a consistent picture of the microscopic dielectric properties of water. The dielectric response presents in the Fourier space a pronounced maximum whose height and position are well established[19–22]. It is possible to model water as a contin-

uous dielectric medium associated with this susceptibility by introducing an appropriate Hamiltonian as a functional of a polarization vector[23]. Within this framework, the contribution of the hydrophobic interaction coming from short-range dipole correlations can be characterized.

In this paper, we introduce a continuous vector model for a polar liquid and we express its free energy as a quadratic Landau-Ginzburg energy function. We derive analytically the corresponding two-point correlation tensor and show that it contains both strong short-range correlations that extend on several nanometers and the van der Waals long-range tail. In a second part, we calculate the fluctuation-induced force between two point-like particles. In a third part we determine the fluctuation-induced interaction between two infinite plates immersed in a correlated dielectric medium. Our approach generates a short-range interaction and a long-range van der Waals attraction. We determine the shape and range of the first one in both cases and discuss its relative importance to the hydrophobic interaction that is measured numerically or experimentally.

II. BULK CORRELATION FUNCTIONS IN A CORRELATED DIPOLAR FLUID

The coarse-grained free energy of a continuous dielectric medium, in the absence of external electric field, can be expressed as a function of its polarization $\mathbf{P}(r)$,

$$\mathcal{H}[\mathbf{P}] = \frac{1}{2}\int d^3r d^3r' \Big[\mathbf{P}(r)\mathbf{K}(r,r')\mathbf{P}(r') + \frac{\nabla\cdot\mathbf{P}(r)\nabla\cdot\mathbf{P}(r')}{4\pi|r-r'|}\Big], \quad (1)$$

where $\mathbf{K}$ is a kernel that encodes the short-range interactions between molecules. The second part of the energy is the long-range dipole-dipole interaction mediated by Coulomb's law. A local kernel $K(r,r') = \delta(r-r')K_0\mathbf{I}$ corresponds to a local dielectric medium with $\epsilon = 1 + K_0^{-1}$. We use units with ϵ_0=1.

With such a formulation it is rather simple to implement the dielectric properties of a medium at semi-microscopic scale. Water is described by a local mean value of the molecular polarization vector averaged over a mesoscopic volume of the liquid. This mean polarization $\mathbf{P}(r)$ is a smooth continuous vector field therefore the free energy of water should allow expansion in powers of the polarization gradient. A systematic approach is to use a Landau-Ginsburg expansion of the free energy for the polarization field. The lower order terms are $\kappa_l(\nabla\cdot\mathbf{P}^2(r))$ and $\kappa_c(\nabla\wedge\mathbf{P}(r))^2$. This expansion is not sufficient to correctly reproduce the behavior of the longitudinal susceptibility $\chi_\parallel$, in particular its pronounced maximum in $q-$space which was determined by molecular dynamics and experiments[20,22]. This illustrates an overresponse of water that can be explained by the structure of the network formed by the hydrogen bounds. A high order term $\alpha(\nabla(\nabla\cdot\mathbf{P}(r)))^2$ is thus added[23]. This gives the following Landau-Ginsburg expansion[23,24]

$$\mathcal{H}[\mathbf{P}] = \frac{1}{2}\int d^3r \Big[K\mathbf{P}^2(r) + \kappa_l(\nabla\cdot\mathbf{P}^2(r)) + \kappa_c(\nabla\wedge\mathbf{P}(r))^2 + \alpha(\nabla(\nabla\cdot\mathbf{P}(r)))^2\Big] + \frac{1}{2}\int d^3r\, d^3r' \frac{\nabla\cdot\mathbf{P}(r)\nabla\cdot\mathbf{P}(r')}{4\pi|r-r'|}. \quad (2)$$

The non local dielectric permitivity of the medium is equal to $\epsilon_{ij}(q) = \delta_{ij} + K_{ij}(q)^{-1}$. The Fourier space longitudinal and transverse dielectric susceptibility associated with this Hamiltonian are

$$\chi_\parallel(q) = 1 - \frac{1}{\epsilon_\parallel(q)} = \frac{1}{1+K+\kappa_l q^2+\alpha q^4}, \quad (3)$$

$$\chi_\perp(q) = \epsilon_\perp(q) - 1 = \frac{1}{K+\kappa_c q^2}, \quad (4)$$

where q denotes the wavevector and $K = \chi^{-1}$ is the zero wavevector static susceptibility of water. The coefficients α and κ_c must be positive for stability at large vectors. The case $\kappa_l < 0$ together with $\alpha > 0$ can qualitatively reproduce the exceptional finite wave-vector response known in water. Its maximum $\chi_\parallel^m = 1/(1+K-\kappa_l^2/(4\alpha))$ is reached for $q = q_0 = \sqrt{\frac{-\kappa_l}{2\alpha}}$. The macroscopic value of dielectric constant, $\epsilon_L(0) = \epsilon_c(0) = 71$, fixes the value of $K = 1/70$. The other parameter values are fixed to reproduce a a wavelength cutoff $1/\lambda_\perp$ equal to 0.5 $\mathring{A}^{-1}$ for the transverse susceptibility and a maximum $\chi_\parallel^m = 40$ for $q \approx 2.6$ $\mathring{A}^{-1}$ for the longitudinal susceptibility[22]. Fig. 1 represents $\chi_\parallel(q)$ and $\chi_\perp(q)$ for $q_0 = 2.6$ $\mathring{A}^{-1}$, $\chi_\parallel^m = 40$ and $\lambda_\perp$ =0.21 nm [22]. The dielectric constant $\epsilon_\parallel(q)$ is linked to the susceptibility via the relation $\epsilon_\parallel(q) = 1/(1-\chi_\parallel(q))$. The correlation between the dipoles is so strong that the dielectric constant becomes negative over a range of wave-vectors[19].

The polarization correlation matrix, $\langle P_i(r)P_j(0)\rangle = G_{ij}(r)$, corresponding to the Hamiltonian Eq. (2) is

$$G_{ij}(r) = \frac{I_1(r)-I_2(r)}{2}\Big(\delta_{ij} - \frac{r_i r_j}{r^2}\Big) + I_2(r)\frac{r_i r_j}{r^2}, \quad (5)$$

where $\langle P(r)P(0)\rangle_\parallel = I_2(r)$ is the longitudinal correlation function and $\langle P(r)P(0)\rangle_\perp = (I_1(r)-I_2(r))/2$ is the transverse correlation function.

The functions $I_1(r)$ and $I_2(r)$ given by:

$$I_1(r) = \frac{e^{-r/\lambda_\perp}}{2\pi K\lambda_\perp^2 r} + \frac{(1+R^2)^2 e^{-r/\lambda_\parallel}}{8\pi(1+K)R\lambda_\parallel^2 r}\sin(r/\lambda_o), \quad (6)$$

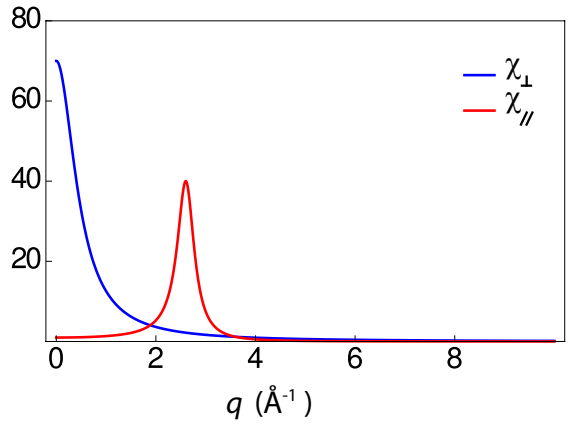

FIG. 1. Longitudinal and transverse susceptibilities. The functions $\chi_\parallel(q)$ and $\chi_\perp(q)$ are given in Eqs. (3,4) and are plotted for $\alpha = 0.021$ Å^4, $\kappa_l = -0.29$ Å^2, $K_c = 0.065$ Å^2, $K = 1/70$. The Hamiltonian parameters are expressed as functions of $(\chi_\parallel^m, q_0, \lambda_\perp)$, $\alpha = \left(1+K-1/\chi_\parallel^m\right)/q_0^4$, $\kappa_l = 2\left(1/\chi_\parallel^m - (1+K)\right)/q_0^2$, $K_c = K/\lambda_\perp^2$ and are calculated for $\chi_\parallel^m$=40, q_0=2.6 Å^{-1} and $\lambda_\perp$=0.21 nm.

and

$$
\begin{aligned}
I_2(r) = &-\frac{e^{-r/\lambda_\perp}}{2\pi K r^2}\left(\frac{1}{\lambda_\perp}+\frac{1}{r}\right)\\
&-\frac{e^{-r/\lambda_\parallel}}{4\pi(K+1)r}\cos\left(\frac{r}{\lambda_o}\right)\left(\frac{2}{r^2}+\frac{1}{r\lambda_o}\left(R+\frac{1}{R}\right)\right)\\
&-\frac{e^{-r/\lambda_\parallel}}{4\pi(K+1)r}\sin\left(\frac{r}{\lambda_o}\right)\left(\frac{1}{\lambda_o^2}\left(\frac{1}{2R^3}+\frac{1}{R}+\frac{R}{2}\right)\right.\\
&\left.+\frac{1}{r}\left(\frac{1}{\lambda_o}+\frac{1}{\lambda_o R^2}\right)+\frac{1}{r^2}\left(\frac{1}{R}-R\right)\right)\\
&+\frac{1}{2\pi K(K+1)r^3},
\end{aligned}
\tag{7}
$$

with $\lambda_\parallel = \sqrt{2}/q_0\sqrt{1/\sqrt{\zeta}-1}$, $\lambda_o = \sqrt{2}/q_0\sqrt{1/\sqrt{\zeta}+1}$, $R = \lambda_\parallel/\lambda_o$ and $\zeta = \alpha q_0^4/(1+K) = \left(1+K-1/\chi_\parallel^m\right)/(1+K)$. Details of calculations are given in Appendix A.

The longitudinal and transverse correlations are the sum of a long-ranged dipolar term that decreases in $1/r^3$ and short-range terms. The correlations can be rewritten as

$$
\langle P(r)P(0)\rangle_\parallel = \frac{1}{2\pi K(K+1)r^3}\left(1+h_\parallel(r)\right) \tag{8}
$$

$$
\langle P(r)P(0)\rangle_\perp = -\frac{1}{4\pi K(K+1)r^3}\left(1+h_\perp(r)\right), \tag{9}
$$

the functions $h_\parallel(r)$ and $h_\perp(r)$ containing the short-range correlations induced by the q-dependence of the susceptibility. Their expression is given in Appendix A. The Fig 2.a, 2.b respectively, represents the correlation functions $\langle P(r)P(0)\rangle_\parallel$ and $\langle P(r)P(0)\rangle_\perp$, the short-range term $h_\parallel(r)$ and $h_\perp(r)$ respectively. The hydrophobic terms $h_\parallel(r)$ and $h_\perp(r)$ are the major contribution to the correlations on the scale of nanometers. We characterize more precisely their shape and range.

The longitudinal decay length $\lambda_\parallel$ and the oscillation length $2\pi\lambda_o$ are functions of $\chi_\parallel^m$ and q_0 and are equal to $\lambda_\parallel$ =0.49 nm and $2\pi\lambda_o$=0.24 nm for the considered set of values. The length $\lambda_\parallel$ increases with $\chi_\parallel^m$. A resonant susceptibility corresponds to a perfect network of hydrogen bonds which is critical and associated with an infinite correlation length. The terms associated with the transverse susceptibility decay exponentially with a characteristic length $\lambda_\perp$ which is fixed to $\lambda_\perp$=0.21 nm. For a nanometric correlation length ($r > \lambda_\parallel$), the envelopes of the oscillating functions $h_\parallel(r)$ and $h_\perp(r)$ are very well approximated by the dominant term $f_\parallel(r) = -KR^3r^2e^{-r/\lambda_\parallel}/4\lambda_\parallel^2$, $f_\perp(r) = -KR^3r^2e^{-r/\lambda_\parallel}/2\lambda_\parallel^2$. The functions $f_\perp(r)$ and $f_\parallel(r)$ reach their maximum values $f_\perp^m = KR^3e^{-2} = 3.9$, $f_\parallel^m = KR^3e^{-2}/2 = 3.0$ for $r = 2\lambda_\parallel = 1.0$ nm. The ranges $r_\parallel^p$ and $r_\perp^p$ on which the hydrophobic terms dominate the long-range contributions are defined as $f_{\parallel,\perp}(r_p)$ =1, they are equal to $r_\parallel^p = 2.6$ nm and $r_\perp^p = 3.1$ nm. The sensitivity of these results as functions of $\chi_\parallel^m$ and q_0 values is given in Appendix C. An increase of $\chi_\parallel^m$ induces an increase in amplitude and range of the short-range terms, a decrease in q_0 induces an increase of their range and has no influence on their amplitudes.

We see that the pronounced maximum of the longitudinal susceptibility generates short-range terms in polarization correlation functions that dominate the van der Waals terms over scales of several nanometers. They extend on a significantly larger distance than the density correlation that was found to vanish over 1 nm[13].

III. INTERACTION BETWEEN POINT-LIKE PARTICLES

Solutes of small size (< 0.5 nm) such as methane induce minor disruptions of the bulk hydrogen-bound network[25]. The perturbation on molecular orientation and dynamics induced by these impurities affect the water molecules of the first hydration layer but the second and further layers conserve the bulk-like properties. In the present approach in which the properties of the fluid are coarse-grained on few layer of water molecules, small inclusions are represented as a point-like variation of the static susceptibility K, see[26].

We consider two microscopic neutral impurities embedded in the fluid at r_1, r_2 respectively and separated by a distance r as represented in Fig. 3.

We write the Hamiltonian $\mathcal{H}_i$ of this system as the Hamiltonian of bulk water given in Eq. (2) in which the macroscopic susceptibility K is modified in r_1 and r_2 and

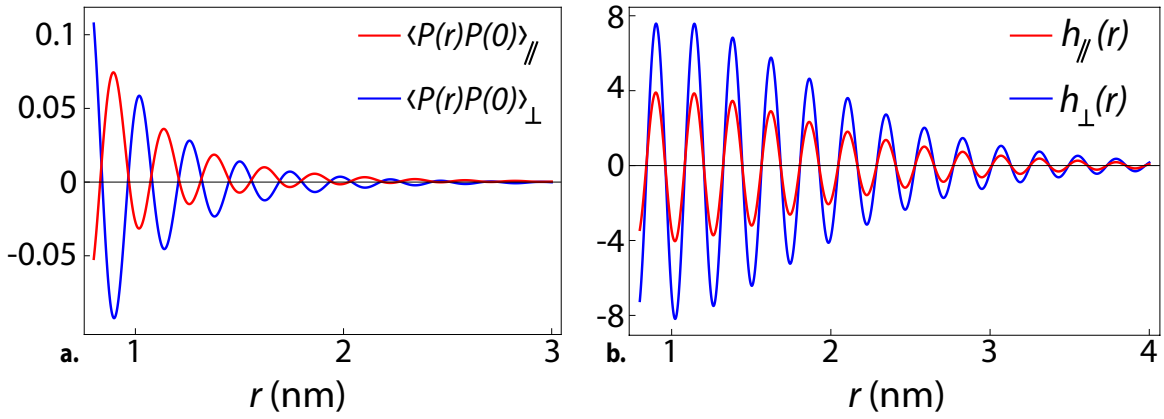

FIG. 2. **a.** Longitudinal $\langle P(r)P(0)\rangle_{\parallel}$ and transverse $\langle P(r)P(0)\rangle_{\perp}$ correlation functions as functions of r (nm). **b.** Longitudinal $h_{\parallel}(r)$ and transverse $h_{\perp}(r)$ short-range correlation terms as a function of the distance r (nm). These functions are plotted here for the set of parameters given in Fig. 1.

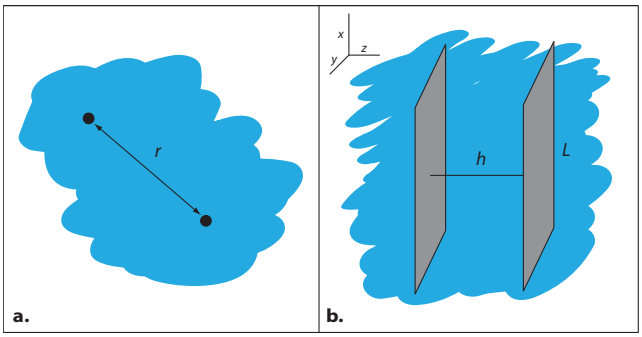

FIG. 3. Interaction of objects immersed in water. **a.** Interaction of two point-like particles separated by a distance r. **b.** Interaction of two macroscopic plates separated by a distance h.

find

$$\begin{aligned}\mathcal{H}_i[\mathbf{P}] =&\frac{1}{2}\int d^3r\Big[K_1\delta(r-r_1)+K_2\delta(r-r_2))\mathbf{P}^2\\&+K\mathbf{P}^2(r)+\kappa_l(\nabla\cdot\mathbf{P}(r))^2+\kappa_c(\nabla\wedge\mathbf{P}(r))^2\\&+\alpha(\nabla(\nabla\cdot\mathbf{P}(r)))^2\Big]\\&+\frac{1}{2}\int d^3rd^3r'\frac{\nabla\cdot\mathbf{P}(r)\nabla\cdot\mathbf{P}(r')}{4\pi|r-r'|}.\end{aligned}\tag{10}$$

The two impurities do not experience any mean-field interaction since the minimum of Eq. (10) occurs at $\mathbf{P}(r)=0$. However, the total free energy of the system which takes into account the fluctuations of the field depends on $r=|r_1-r_2|$ generating a Casimir-like interaction between the two particles. An abundant literature reports theoretical studies of inclusion interactions in correlated fluids or membranes (see[27] for a review) and the steps of the analytic derivation of this interaction are well established. The partition function of the system

$$\mathcal{Z}_i=\int\mathcal{D}Pe^{-\beta\mathcal{H}_i[P]},\tag{11}$$

is rewritten by performing a Hubbard-Stratonovich transformation

$$\begin{aligned}\mathcal{Z}_i=&\int\mathcal{D}P\int\Pi_{j=1,2}\mathcal{D}h_je^{-\frac{\beta}{2}\int d^3rK_j\delta(r-r_j)\left(\frac{h_j^2}{K_j}+2i\frac{h_j}{K_j}P(r)\right)}\\&e^{-\frac{\beta}{2}\int d^3rKP^2+\kappa_l(\nabla P(r))^2+\kappa_c(\nabla\wedge\mathbf{P}(r))^2+\alpha(\nabla\cdot\nabla P(r))^2}\\&+e^{-\frac{\beta}{2}\int d^3r\int d^3r'\frac{\nabla P(r)\nabla P(r')}{|r-r'|}},\end{aligned}\tag{12}$$

where h_1 and h_2 are two auxiliary fields. Then calculating the Gaussian integrals yields

$$\mathcal{Z}_i\propto 1/\det\begin{pmatrix}\mathbf{I}/K_1+\mathbf{G}(0) & \mathbf{G}(r_2-r_1)\\ \mathbf{G}(r_1-r_2) & \mathbf{I}/K_2+\mathbf{G}(0)\end{pmatrix}^{1/2},\tag{13}$$

in which the above 6×6 matrix, made of four 3×3 blocks, involves the identity tensor $\mathbf{I}$ and the Green function matrix $\mathbf{G}(r_1-r_2)$ given in Eq. (5). The total free energy of individual impurities in water is defined as $F_i(r)=-k_bT\ln Z_i(r)$. In the following we will only consider the interaction between the two particles that vanishes when $r=|r_1-r_2|\to\infty$. It is obtained by subtracting the free energy of the system in which the two impurities are too far apart to interact, *i. e.* for vanishing $\mathbf{G}(r)$ and gives

$$F_{int}(r)=\frac{k_bT}{2}\ln\det\mathbf{M}(r),\tag{14}$$

with

$$\mathbf{M}(r)=\begin{pmatrix}\mathbf{I} & \mathbf{G}(r)(\frac{\mathbf{I}}{K_1}+\mathbf{G}(0))^{-1}\\ \mathbf{G}(r)(\frac{\mathbf{I}}{K_2}+\mathbf{G}(0))^{-1} & \mathbf{I}\end{pmatrix}.\tag{15}$$

The Green's function diverges in $r = 0$ and one has to introduce a short-range cutoff Λ to calculate the interaction free energy, $F_{int}(r)$. This takes into account that the impurities are not punctual but have a spacial expansion. This cutoff Λ is thus the radius of the impurity. The dielectric susceptibility variation K_i, defined in Eq (10) is induced by the inclusion and scales as $1/L^3$. It can be estimated as the difference between the macroscopic susceptibility of water K and the macroscopic susceptibility of the impurity material K_b divided by the inclusion volume, *i. e.* $K_i(\Lambda) = (K_b - K)/(4/3\pi\Lambda^3)$. We verify that the introduction of this microscopic cutoff gives correct results for macroscopic thermodynamics values associated with the system. To do so, we calculate the free energy of two inclusions embedded in water when the separation distance between them goes to infinity. In this case, the interaction energy vanishes and F_i is equal to twice the inclusion solvation energy. Using Eq. (14), we obtain the following expression for the solvation energy,

$$E_{s,i} = -\frac{k_bT}{4}\mathrm{lndet}\mathbf{M}_\infty \tag{16}$$

with

$$\mathbf{M}_\infty = \begin{pmatrix} \mathbf{I}/K_1(\Lambda) + \mathbf{G}(\Lambda) & 0 \\ 0 & \mathbf{I}/K_2(\Lambda) + \mathbf{G}(\Lambda) \end{pmatrix}. \tag{17}$$

For two molecules of methane, (*i. e.* $\Lambda = 2\mathring{A}$ and $K_b = 1$), we find $E_{s,i}$ =3.37 k_bT (*i. e.* 2 kcal.mol^{-1}) which is in excellent agreement with the tabulated values[14]. We now calculate the interaction energy between two methane molecules. Using the relation $\ln\det\mathbf{M} = \mathrm{Tr}\ln\mathbf{M}$ and expanding $\ln\mathbf{M}$ to second order in $\mathbf{G}(r)(\frac{\mathbf{I}}{K_i} + \mathbf{G}(0))^{-1}$ we obtain,

$$\frac{F_{int}(r)}{k_bT} = -\frac{1}{2}\mathrm{Tr}\left(\mathbf{G}(r)\cdot\left(\frac{\mathbf{I}}{K_1(\Lambda)} + \mathbf{G}(\Lambda)\right)^{-1}\cdot\mathbf{G}(r)\cdot\left(\frac{\mathbf{I}}{K_2(\Lambda)} + \mathbf{G}(\Lambda)\right)^{-1}\right) \tag{18}$$

$$= -\frac{1}{2}\left(2\left(\frac{(I_1(r) - I_2(r))/2}{1/K_1(\Lambda) + (I_1(\Lambda) - I_2(\Lambda))/2}\right)^2 + \left(\frac{I_2(r)}{1/K_1(\Lambda) + I_2(\Lambda)}\right)^2\right). \tag{19}$$

In Eq. (19), we have used the expression of $\mathbf{G}(r)$ given in Eq. (5). This interaction is attractive. We plot the dimensionless term $F_{int}(r)/k_bT$ and its van der Waals contribution $F_{int}^{vdW}(r)$ (obtained for $h_\parallel(r) = 0$, $h_\perp(r) = 0$) in Fig. 4. As expected, the long-range interaction decays in $1/r^6$. The short-range contribution is an oscillating term that exponentially decreases and vanishes on 1.5 nm. It represents the dominant term of the interaction for separation distances inferior to 1 nm and its amplitude is a fraction of k_bT on this range. The decay length λ_{point} of the envelope is numerically evaluated to λ_{point}=0.32 nm ± 0.01 nm. These results are in very good agreement with ones obtained using different molecular fields theory of water[28,29]. As a conclusion of this part, we can say that our model captures the essential features for hydrophobic interaction between punctual objects.

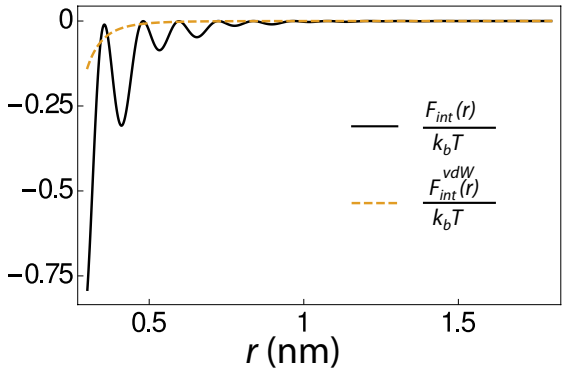

FIG. 4. Interaction energy $F_{int}(r)/k_bT$in k_bT units between two methane molecules immersed in water and separated by a distance r. The dashed line represents the van der Waals contribution $F_{int}(r)^{vdW}/k_bT$ of the interaction energy. The plots are obtained for $K_b = 1$ and $\Lambda = 2$ Å.

IV. INTERACTION BETWEEN MACROSCOPIC NEUTRAL OBJECTS

In this section, we aim to characterize the short-range part of the fluctuation-induced interaction between macroscopic objects. Unlike small molecules that do not perturb the network of hydrogen bounds in water, a preferential molecular orientation is induced by extended objects which tend to align the molecule planes with their surfaces. This feature is due to the tendency for water molecules to maximize the number of hydrogen bounds under the geometrical constraint of the interface. As a consequence of this constrained orientation, a non vanishing surface electrostatic potential is observed at the surface of hydrophobic plates. It is generated by the interaction between water molecule partial charges and their image partial charges[7]. Moreover, theoretical models and molecular dynamics simulations report that water density is reduced at the surface of extended objects on

a layer of few $\mathring{A}$[7,25].

We consider two plates of lateral size L immersed in the fluid and localized in $z = 0$ and $z = h$ (see Fig. 3). The separation distance h is much smaller than the lateral extension. The interaction between the plates and the fluid leads to a mean polarization $\mathbf{P_m}$ such that the field in the medium can be written as this mean polarization perturbed by fluctuations $\mathbf{P} = \mathbf{P_m} + \delta\mathbf{P}$. The orientational effect of hydrophobic objects on water molecules plays a role in the two first hydration layers and vanish for few $\mathring{A}$ apart from the surface. We will neglect such mean polarization effects in the following.

In the present coarse-grained approach, the mean field and consequently the mean field induced interaction vanish. The interaction between the two plates is a Casimir-like interaction induced by the constraints on $\delta\mathbf{P}$. To calculate this fluctuating interaction we follow[8,9]. We first expend the Hamiltonian of a system around the mean polarization field $\mathbf{P_m}$. We find

$$\mathcal{H}_P[\delta\mathbf{P}] = \frac{1}{2}\int d^3r d^3r'\, \delta\mathbf{P}(r)\mathbf{G}^{-1}(r-r')\delta\mathbf{P}(r'), \quad (20)$$

where $\mathbf{G}(r-r')$ is the two-point correlation tensor given in Eq. (5). The fluctuation-induced interaction between two plates is obtained by integrating over all the configurations of the vector field $\delta\mathbf{P}$ that satisfy the constraints imposed by the plates. The fluctuating polarization field can be decomposed in a longitudinal and a transverse part as,

$$\delta\mathbf{P}(r) = \nabla\delta\psi(r) + \nabla\wedge\delta\mathbf{A}(r) \quad (21)$$

where $\nabla\delta\psi(r)$ is the longitudinal part of the fluctuating polarization which is linked to the fluctuating part of the electrostatic potential $\delta\psi_e(r)$ by the relation $\nabla\delta\psi(r) = -\int d^3r'\chi_\parallel(r,r')\nabla\delta\psi_e(r)$, where $\chi_\parallel(r,r')$ is the longitudinal dielectric susceptibility of water. The fluctuating transverse part of the polarization is written as a function of the potential vector $\nabla\wedge\mathbf{A}$. The interaction between the fluid and the surface has to be expressed in terms of boundary conditions on the fluctuating fields. However, this interaction is difficult to model since it includes many effects. We consider metallic boundary conditions that freeze the fluctuations of the potential $\psi(r)$ from which derives the polarization *i.e.* $\delta\psi(r_\alpha(x_\alpha)) = 0$ where $r_\alpha(x_\alpha)$ ($\alpha = 1, 2$) are the coordinates of the plates. The interaction induced by frozen polarization fluctuations was also considered and its calculation is given in Appendix B. Both boundary condition generates a specific long-range interaction that models either the interaction between thin dielectric plates in $1/r^4$ (frozen $\delta\mathbf{P}$) or the interaction between thin metallic plates or thick plates in $1/r^2$ (frozen $\delta\psi$)[30].

The free energy of bulk water can be written as the sum of a longitudinal and a transverse contribution,

$$\mathcal{H}_P[\delta\psi,\delta\mathbf{A}] = \frac{1}{2}\Big(\int drdr'\,\delta\psi(r)K_\psi(r-r')\delta\psi(r') + \int drdr'\,\delta\mathbf{A}(r)\mathbf{K_A}(r-r')\delta\mathbf{A}(r')\Big) \quad (22)$$

with

$$K_\psi^{-1}(r) = \frac{1}{(2\pi)^3}\int d^3q\, e^{iqr}\frac{1}{q^2}\mathrm{Tr}\mathbf{G}(q).\frac{q\times q}{q^2}, \quad (23)$$

$$\mathbf{K_A}^{-1}(r) = \frac{1}{(2\pi)^3}\int d^3q\, e^{iqr}\frac{1}{q^2}\mathbf{G}(q).(\mathbf{I}-\frac{q\times q}{q^2}). \quad (24)$$

We freeze the fluctuations of the electrostatic potential on the plates, in $z = 0$ and $z = h$, and do not impose any condition on the fluctuations of $\mathbf{A}$. As a consequence, the free energy of the system depends on h through the first term of the Hamiltonian given in Eq. (22), the second term does not contribute to the Casimir-like interaction between the plates and we will not consider it in the following. The partition function of the system is given by

$$\mathcal{Z}_\psi[\delta\psi] = \int\mathcal{D}[\delta\psi]\Pi_{\alpha=1,2}\delta(\delta\psi(r_\alpha)) \times e^{-\frac{\beta}{2}\int d^3rd^3r'\delta\psi(r)G_\psi^{-1}(r-r')\delta\psi(r')} \quad (25)$$

with $G_\psi^{-1}(r-r') = K_\psi(r-r')$ defined in Eq. (23). Using the integral representation of the δ function, we obtain,

$$\mathcal{Z}_\psi[\delta\psi] = \int\mathcal{D}[\delta\psi]\int\Pi_{\alpha=1,2}\mathcal{D}C_\alpha e^{i\Sigma_{\alpha=1,2}\int d^2x_\alpha C_\alpha(x)\delta\psi(r_\alpha(x_\alpha))} \times e^{-\frac{\beta}{2}\int d^3rd^3r'\delta\psi(r)G_\psi^{-1}(r-r')\delta\psi(r')} \quad (26)$$

where C_α are auxiliary fields defined on the plates acting as sources coupled to the fluctuating electrostatic potential. Writing $\Sigma_{\alpha=1,2}\int d^2x_\alpha C_\alpha(x_\alpha)\delta\psi(r_\alpha(x_\alpha)) = \int d^3r\delta\psi(r)J(r)$, with $J(r) = \Sigma_{\alpha=1,2}\int d^2x_\alpha C_\alpha(x_\alpha)\delta(r-r_\alpha)$ and calculating all the Gaussian integrals yields

$$\mathcal{Z}_\psi[\delta\psi] = \frac{(2\pi)^{N/2}}{\sqrt{\left|G_\psi^{-1}(r-r')\right|}}\frac{(2\pi)^{M/2}}{\sqrt{|M_\psi(r_1-r_2)|}} \quad (27)$$

where $G_\psi(r-r') = K_\psi^{-1}(r-r')$ is given in Eq. (23), r_1 and r_2 are the coordinates of the plates and $M_\psi(r_1-r_2)$ is

$$\mathbf{M}_\psi = \begin{pmatrix} G_\psi(x-x',y-y',0) & G_\psi(x-x',y-y',-h) \\ G_\psi(x-x',y-y',h) & G_\psi(x-x',y-y',0)\end{pmatrix}.$$

The free energy of the system is defined as $F_\psi(h) = -k_bT\ln\mathcal{Z}_\psi$. The interaction energy is obtained by subtracting the energy of the system in which the two plates do not interact, *i.e.* for vanishing $G_\psi(r)$. This gives

$$\frac{F_{int,\psi}(h)}{L^2k_bT} = \frac{1}{2}\int\frac{dpd\theta p}{4\pi^2}\ln\begin{vmatrix} 1 & \frac{G_\psi(p,\theta,h)}{G_\psi^{-1}(p,\theta,0)} \\ \frac{G_\psi(p,\theta,h)}{G_\psi^{-1}(p,\theta,0)} & 1\end{vmatrix} \quad (28)$$

where $G_\psi(z,p)$ (with $p = \sqrt{q_x^2+q_y^2}$) is equal to $1/2\pi \int_{-\infty}^{\infty} dq_z K_\psi^{-1}(q) e^{iq_z z}$. Its expression is

$$G_\psi(z,p) = \frac{e^{-ph}}{2(K+1)p} + \frac{e^{-\gamma(p)h}}{(\delta^2(p)+\gamma^2(p))\sqrt{1/\zeta-1}} \times \Big(\Big(\delta(p) - \gamma(p)\sqrt{1/\zeta-1}\Big)\cos(\delta(p)h) + (\gamma(p)+\delta(p)\sqrt{1/\zeta-1})\sin(\delta(p)h)\Big) \quad (29)$$

with $\delta(p) = \sqrt{\frac{q_0^2-p^2+\sqrt{p^4-2q_0^2p^2+q_0^4/\zeta}}{2}}$ and $\gamma(p) = \sqrt{\frac{-q_0^2+p^2+\sqrt{p^4-2q_0^2p^2+q_0^4/\zeta}}{2}}$.

The integral over p given in Eq. (28) is performed numerically. The interaction energy $\frac{E_{int,\psi}}{L^2 k b_T}(h)$ is represented in Fig. 5 in solid line, the dashed line corresponds to $\frac{E_{int}^{vdW}}{L^2 k_b T} = -\frac{\zeta(3)}{16\pi h^2}$, the pure van der Waals contribution. As shown in Fig. 5., the long-range interaction resulting from frozen electrostatic field fluctuations is equal the van der Waals interaction. An additional short-range attractive interaction is observed at for $h < 1.5$ nm, we identify this attraction as a part of the 'true' hydrophobic interaction generated here by the constrained dipole fluctuations. This contribution dominates the van der Walls interaction on 1 nm with an amplitude of 0.1 nm^{-2}, *i. e.* around an order of magnitude smaller than the interaction energy extrapolated from measurement at larger distances[6]. This short-range term decays exponentially with a characteristic length $\lambda_{plate} = 0.17$ nm ± 0.01 nm and vanishes on 1.5 nm, these results deviate from the experimental measurements by about a factor 5.

In conclusion, our model generates an exponentially decaying short-range interaction that dominates the van der Walls interaction on small separation distances. This is in qualitative agreement with the experiments. However our predictions underestimate the range and the amplitude of the interaction by a factor 5 to 10, confirming that density effects, that we have neglected here, are preponderant for objects of large size[6,29].

V. DISCUSSION

The hydrophobic interaction between macroscopic objects has been extensively studied experimentally over a period of 30 years. The recent understanding of the origin of surprising long-range interactions has allowed one to refocus on the 'true' hydrophobic interaction. New experimental methods redefine it as a short-range attraction that overpowers van der Waals interaction over few nanometers. This effect is presumed to be of primary importance in biology and nanoscale assembly and its modelization remains a challenge.

Structural and thermodynamics aspects of hydrophobic hydration are reasonably well understood[14,31], density functional theories for water have successfully modeled the solvation including a non trivial size-solute dependence[15]. They are also able to describe rare fluctuation events that could be responsible for hydrophobic association of two plates separated by few $\mathring{A}$ by removing all the water molecules between these plates. An evaluation of the range of attraction between hydrophobic objects is more difficult with this method because the long-range van der Waals terms are not explicitly taken into account.

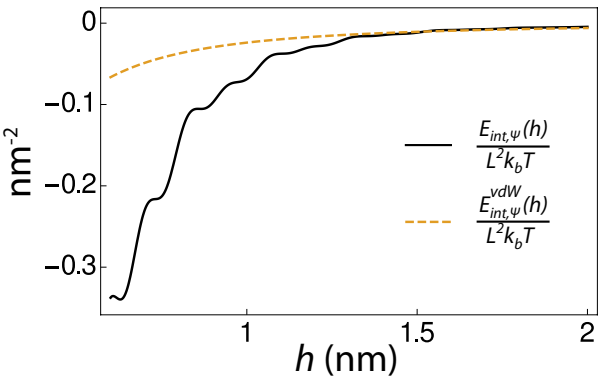

FIG. 5. Interaction $\frac{E_{int,\psi}}{L^2 k_b T}(h)$ between two plates immersed in water. The dashed line represents the van der Waals contribution $\frac{E_{int}^{vdW}}{L^2 k_b T}(h)$ of the interaction. The interaction is plotted for the same parameter values as in Fig. 1.

In this paper, we have described water as a continuous dielectric medium, characterized by a vectorial order parameter, the polarization field $\mathbf{P}$ and a free energy which reproduces correctly the remarkable dielectric properties of the fluid. In the frame of this model, we have characterized the range of the correlations and evaluated the distance on which short-range terms dominate van der Waals long-range terms. We have first calculated the two point-correlation tensor and have shown that the short-range part of polarization correlations is the dominant contribution on about 3 nm, *i. e.* on large distances when compared to density fluctuations that vanish on 1 nm. We have calculated the interactions between small and macroscopic objects and evaluated the range and decay of the hydrophobic contribution. We have found that this interaction extends in both cases on about 1.5 nm. Whereas the interaction presents pronounced oscillations for point-like objects, the oscillations are smoothed for macroscopic objects and the interaction is exponentially decaying. This qualitative difference is in agreement with molecular dynamics results which are obtained for microscopic plates and report oscillating interactions, and experiments which measure interaction between macroscopic plates and mention smooth exponentially decaying attraction[5,12]. The crossover between the two regimes is estimated to be for an impurity size of 1 nm[32]. This could be estimated with our model by calculating numerically interactions between spheres of increasing radius. The exponential decay length of the interaction is larger for point-like objects (λ_{point}=0.32 nm) than for macroscopic

objects ($\lambda_{plate} = 0.17$ nm).

Whereas our model generates an interaction between punctual objects that is in very good agreement with existing results, the interaction between large objects is significantly underestimated. The small sensitivity of our results as a function of the shape of the dielectric susceptibility excludes a deviation due to a miss-estimation of dielectric properties of water. A description of the hydrophobic interaction as a fluctuation-induced force generated by both density and polarization fluctuations could be envisaged to to better reproduce experimental observations[20].

In conclusion, the model we propose reproduces qualitatively recent simulation and experimental results on hydrophobic forces. It allows analytic calculations for dipole fluctuation-induced interactions between objects of simple geometry and the numerical implementation for systems of more complicated geometries seems possible. Therefore we believe it could be useful to investigate the strength of hydrophobic interactions between biological objects.

ACKNOWLEDGMENTS

Work in part supported by ANR grant FSCF.

Appendix A: Green function in real space

In this Appendix, we calculate the longitudinal and transverse correlations of polarization. We characterize their amplitude and range.

The expression of the two-point correlation tensor in the Fourier space,

$$G_{ij}(q) = \frac{1}{K + K_c q^2}\left(\delta_{ij} - \frac{q_i q_j}{q^2}\right) + \frac{1}{1 + K + \kappa_l q^2 + \alpha q^4}\frac{q_i q_j}{q^2}, \quad \text{(A1)}$$

is easily deduced from the free energy given in Eq. (2). The expression of the Green's function in the real space is given by

$$G_{ij}(r) = \int_0^\infty \frac{q^2 dq}{2\pi^3}\int_0^{2\pi} d\theta \int_0^\pi d\phi \sin(\phi) G_{ij}(q) e^{iqr\cos(\phi)}. \quad \text{(A2)}$$

The tensorial product $\frac{q_i q_j}{q^2}$ can be expressed in spherical coordinates (q, θ, ϕ),

$$\frac{q \times q}{q^2} = \begin{pmatrix} \cos(\theta)\sin^2(\phi) & \cos(\theta)\sin(\theta)\sin(\phi) & \cos(\theta)\sin(\phi)\cos(\phi) \\ \cos(\theta)\sin(\theta)\sin(\phi) & \sin^2(\theta)\sin^2(\phi) & \sin(\theta)\sin(\phi)\cos(\phi) \\ \cos(\theta)\sin(\phi)\cos(\phi) & \sin(\theta)\sin(\phi)\cos(\phi) & \cos^2(\phi) \end{pmatrix}.$$

After integration on θ, two integrals remain to be calculated:

$$I_1(r) = \frac{1}{(2\pi)^2}\int_0^\pi d\phi \int_0^\infty dq e^{iqr\cos(\phi)}\Big(\frac{2}{K + K_c q^2} + \frac{1}{\alpha q^4 + \kappa_l q^2 + (K+1)}\Big) q^2 \sin(\phi), \quad \text{(A3)}$$

and

$$\begin{aligned} I_2(r) =& \frac{1}{(2\pi)^2}\int_0^\pi d\phi \int_0^\infty dq \frac{1}{K + K_c q^2} e^{iqr\cos(\phi)} q^2 \sin(\phi) \\ &+ \left(\frac{1}{1 + K + \kappa_l q^2 + \alpha q^4} - \frac{1}{K + K_c q^2}\right) \\ &\times \cos^(\phi) e^{iqr\cos(\phi)} q^2 \sin(\phi) \quad \text{(A4)} \\ =& \frac{1}{(2\pi)^2}\int_0^\pi d\phi \int_0^\infty dq \frac{1}{K + K_c q^2} e^{iqr\cos(\phi)} q^2 \sin(\phi) \\ &+ \frac{d^2}{dr^2}\frac{1}{(2\pi)^2}\int_0^\pi d\phi \int_0^\infty dq \Big(\frac{1}{1 + K + \kappa_l q^2 + \alpha q^4} \\ &- \frac{1}{K + K_c q^2}\Big) e^{iqr\cos(\phi)} \sin(\phi). \quad \text{(A5)} \end{aligned}$$

These integrals are performed using the residue theorem giving:

$$I_1(r) = \frac{e^{-r/\lambda_\perp}}{2\pi K \lambda_\perp^2 r} + \frac{(1+R^2)^2 e^{-r/\lambda_\parallel}}{8\pi(1+K)R\lambda_\parallel^2 r}\sin(r/\lambda_o), \quad \text{(A6)}$$

$$\begin{aligned} I_2(r) =& -\frac{e^{-r/\lambda_\perp}}{2\pi K r^2}\left(\frac{1}{\lambda_\perp} + \frac{1}{r}\right) \\ &- \frac{e^{-r/\lambda_\parallel}}{4\pi(K+1)r}\cos\left(\frac{r}{\lambda_o}\right)\left(\frac{2}{r^2} + \frac{1}{r\lambda_o}\left(R + \frac{1}{R}\right)\right) \\ &- \frac{e^{-r/\lambda_\parallel}}{4\pi(K+1)r}\sin\left(\frac{r}{\lambda_o}\right)\left(\frac{1}{\lambda_o^2}\left(\frac{1}{2R^3} + \frac{1}{R} + \frac{R}{2}\right)\right. \\ &\left. + \frac{1}{r}\left(\frac{1}{\lambda_o} + \frac{1}{\lambda_o R^2}\right) + \frac{1}{r^2}\left(\frac{1}{R} - R\right)\right) \\ &+ \frac{1}{2\pi K(K+1)r^3}. \quad \text{(A7)} \end{aligned}$$

with $\lambda_\perp = \sqrt{\frac{K_c}{K}}$, $\lambda_\parallel = \frac{\sqrt{2}}{q_0\sqrt{1/\sqrt{\zeta}-1}}$, $\lambda_o = \frac{\sqrt{2}}{q_0\sqrt{1/\sqrt{\zeta}+1}}$, $R = \frac{\lambda_\parallel}{\lambda_o}$ and $\zeta = \frac{\alpha q_0^4}{1+K} = \frac{1}{1+K}\left(1 + K - \frac{1}{\lambda_\parallel^m}\right)$.
The Green function can be written as

$$G_{ij}(r) = \begin{pmatrix} \frac{I_1(r)-I_2(r)}{2} & 0 & 0 \\ 0 & \frac{I_1(r)-I_2(r)}{2} & 0 \\ 0 & 0 & I_2(r) \end{pmatrix}, \quad \text{(A8)}$$

in the intrinsic spherical basis. After a basis change, the two-point correlation tensor is:

$$G_{ij}(r) = \frac{I_1(r) - I_2(r)}{2}(\delta_{ij} - \frac{r_i r_j}{r^2}) + I_2(r)\frac{r_i r_j}{r^2}, \quad \text{(A9)}$$

where $\langle P(r)P(0)\rangle_{\parallel} = I_2(r)$ is the longitudinal correlation and $\langle P(r)P(0)\rangle_{\perp} = \frac{I_1(r)-I_2(r)}{2}$ the transverse correlation. The longitudinal and transverse correlation functions can be written as:

$$\langle P(r)P(0)\rangle_{\parallel} = \frac{1}{2K(K+1)r^3}\left(1+h_{\parallel}(r)\right), \tag{A10}$$

$$\langle P(r)P(0)\rangle_{\perp} = \frac{-1}{4K(K+1)r^3}\left(1+h_{\perp}(r)\right), \tag{A11}$$

where the functions $h_{\parallel}(r)$ and $h_{\perp}(r)$ contain the short-range terms. Their expression is:

$$\begin{aligned} h_{\parallel}(r) =& e^{-r/\lambda_{\perp}}(K+1)r^2\left(\frac{1}{r\lambda_{\perp}}+\frac{1}{r^2}\right) \\ & -\frac{e^{-r/\lambda_{\parallel}}}{2}Kr^2\Bigg(\cos(\frac{r}{\lambda_o})\left(\frac{2}{r^2}+\frac{1}{r\lambda_o}\left(R+\frac{1}{R}\right)\right) \\ & +\sin(\frac{r}{\lambda_o})\Bigg(\frac{1}{\lambda_o^2}\left(\frac{1}{2R^3}+\frac{1}{R}+\frac{R}{2}\right)+\frac{1}{r\lambda_o}\left(1+\frac{1}{R^2}\right) \\ & +\frac{1}{r^2}\left(\frac{1}{R}+R\right)\Bigg)\Bigg) \end{aligned} \tag{A12}$$

and

$$\begin{aligned} h_{\perp}(r) =& e^{-r/\lambda_{\perp}}(K+1)r^2\left(\frac{1}{\lambda_{\perp}^2}+\frac{1}{r\lambda_{\perp}}+\frac{1}{r^2}\right) \\ & -\frac{e^{-r/\lambda_{\parallel}}}{2}Kr^2\Bigg(\cos(\frac{r}{\lambda_o})\left(\frac{2}{r^2}+\frac{1}{r\lambda_o}\left(R+\frac{1}{R}\right)\right) \\ & +\sin(\frac{r}{\lambda_o})\Bigg(\frac{1}{\lambda_o^2}\left(\frac{1}{R^3}+\frac{2}{R}+R\right)+\frac{1}{r\lambda_o}\left(1+\frac{1}{R^2}\right) \\ & -\frac{1}{r^2}(R-\frac{1}{R})\Bigg)\Bigg). \end{aligned} \tag{A13}$$

Appendix B: Fluctuation-induced force between two plates that freeze polarization fluctuations

In this Appendix, we calculate the fluctuation-induced force between two plates located in $z=0$ and $z=h$ that impose frozen polarization fluctuations on their boundaries. To do so we calculate the h-dependent contribution of the system's free energy. The partition function of the system is written as

$$\begin{aligned} \mathcal{Z}_P = & \int \mathcal{D}\mathbf{P}\Pi_{\alpha=1,2}\delta(\delta\mathbf{P}(\mathbf{r}_\alpha)) \\ & \times e^{\frac{1}{2}\int d^3r d^3r' \delta\mathbf{P}(r)\mathbf{G}^{-1}(r-r')\delta\mathbf{P}(r')}. \end{aligned} \tag{B1}$$

Using the integral representation of δ function, we obtain,

$$\begin{aligned} \mathcal{Z}_P = & \int \mathcal{D}\delta\mathbf{P}\int \Pi_{\alpha=1,2}\mathcal{D}\mathbf{C}_\alpha e^{i\Sigma_{\alpha=1,2}\int d^2x_\alpha \mathbf{C}_\alpha(x)\delta\mathbf{P}(r_\alpha(x_\alpha))} \\ & + e^{-\frac{\beta}{2}\int d^3r d^3r' \delta\mathbf{P}(r)\mathbf{G}^{-1}(r-r')\delta\mathbf{P}(r')}, \end{aligned} \tag{B2}$$

where $\mathbf{C}_\alpha$ are vectorial auxiliary fields defined on the plates acting as sources coupled to the polarization. Writing $\Sigma_{\alpha=1,2}\int d^2x_\alpha \mathbf{C}_\alpha(x_\alpha)\delta\mathbf{P}(r_\alpha(x_\alpha)) = \int d^3r \delta\mathbf{P}(r)\mathbf{J}(r)$, with $\mathbf{J}(r) = \Sigma_{\alpha=1,2}\int d^2x_\alpha \mathbf{C}_\alpha(x_\alpha)\delta(r-r_\alpha)$ and performing the Gaussian integrals over $\delta\mathbf{P}$ and $\mathbf{C}_\alpha$ we find,

$$\mathcal{Z}_P = \frac{(2\pi)^{N/2}}{\sqrt{|G^{-1}(r-r')|}}\frac{(2\pi)^{M/2}}{\sqrt{|M_P(r_1-r_2)|}}, \tag{B3}$$

where $G(r-r')$ is the bulk function given in Eq. (5), r_1 and r_2 are the coordinates of the plates and $M_p(r_1-r_2)$ is

$$\mathbf{M}_P = \begin{pmatrix} \mathbf{G}(x-x',y-y',0) & \mathbf{G}(x-x',y-y',-h) \\ \mathbf{G}(x-x',y-y',h) & \mathbf{G}(x-x',y-y',0) \end{pmatrix}. \tag{B4}$$

The free energy F_P of the system is defined as $F_P(h) = -k_bT\ln\mathcal{Z}_P$. The interaction energy is obtained by subtracting the energy of the system in which the two plates are too far apart to interact. The interaction energy between the plates is equal to

$$E_{int,P}(h) = \frac{k_BT}{2}\int dxdx'dydy' \ln|M_{p,int}|. \tag{B5}$$

with

$$M_{int,P} = \begin{pmatrix} \mathbf{I} & \mathbf{G}(x-x',y-y',h).\mathbf{G}^{-1}(x-x',y-y',0) \\ \mathbf{G}(x-x',y-y',-h).\mathbf{G}^{-1}(x-x',y-y',0) & \mathbf{I} \end{pmatrix}. \tag{B6}$$

This equation can be Fourier-transformed to obtain:

$$E_{int,P}(h) = \frac{L^2k_BT}{2}\int_0^\infty dp\int_0^{2\pi} d\theta \frac{1}{4\pi^2}p\ln\left|\tilde{M}_{p,int}\right|, \tag{B7}$$

where

$$\tilde{M}_{int,P} = \begin{pmatrix} \mathbf{I} & \tilde{\mathbf{G}}(p,\theta,h).\tilde{\mathbf{G}}^{-1}(p,\theta,0) \\ \tilde{\mathbf{G}}(p,\theta,-h).\tilde{\mathbf{G}}^{-1}(p,\theta,0) & \mathbf{I} \end{pmatrix},$$

with

$$\tilde{\mathbf{G}}(p,\theta,z) = \frac{1}{2\pi}\int_{-\infty}^{\infty} dq_z \mathbf{G}(p,q_z)e^{iq_{zz}}. \qquad \text{(B8)}$$

Using the relation $\ln \mathrm{Det A} = \mathrm{Tr} \ln \mathrm{A}$, and after an expansion at the second order in $\tilde{\mathbf{G}}\tilde{\mathbf{G}}^{-1}$, the interaction energy can be expressed as,

$$\begin{aligned}\frac{E_{int,P}(h)}{k_bT} = & \frac{1}{2}\int_0^{\infty} dp \int_0^{2\pi} d\theta p \frac{1}{4\pi^2}\mathrm{Tr}(\tilde{\mathbf{G}}^{-1}(p,\theta,0)\tilde{\mathbf{G}}(p,\theta,h) \\ \times & \quad \tilde{\mathbf{G}}^{-1}(p,\theta,0)\tilde{\mathbf{G}}(p,\theta,h)).\end{aligned} \qquad \text{(B9)}$$

The matrix $\tilde{\mathbf{G}}(p,\theta,z)$ is written as

$$\tilde{G}(p,\theta,z) = \begin{pmatrix} F_1(p,z)+F_2(p,z)\cos^2(\theta) & F_2(p,z)\cos(\theta)\sin(\theta) & F_3(p,z)\cos(\theta) \\ F_2(p,z)\cos(\theta)\sin(\theta) & F_1(p,z)+F_2(p,z)\sin^2(\theta) & F_3(p,z)\sin(\theta) \\ F_3(p,z)\cos(\theta) & F_3(p,z)\sin(\theta) & F_1(p,z)+F_4(p,z) \end{pmatrix}, \qquad \text{(B10)}$$

with

$$\begin{aligned} F_1(p,z) &= \frac{e^{(-\sqrt{K/Kc+p^2}z)}}{2K_c\sqrt{K/Kc+p^2}}, \\ F_{2h}(p,z) &= \frac{1}{2(1+K)}\Big(\frac{e^{-pz}}{p} + \frac{e^{-\gamma(p)h}}{(\delta^2(p)+\gamma^2(p))\sqrt{\frac{1}{\zeta}-1}}\left(\delta(p)-\gamma(p)\sqrt{\frac{1}{\zeta}-1}\right)\cos(\gamma(p)z) \\ &\quad + (\gamma(p)+\delta(p))\sin(\gamma(p)z)\Big) - \frac{1}{2K}\left(\frac{e^{-pz}}{z} - \frac{e^{-\sqrt{K/Kc+p^2}h}}{\sqrt{K/Kc+p^2}}\right), \end{aligned} \qquad \text{(B11)}$$

and $F_3(p,z) = -ip\partial_z F_2(p,z)$, $F_4(p,z) = -\partial_z^2 F_2(p,z)$, where $\gamma(p) = \sqrt{\frac{q_0^2-p^2+\sqrt{p^4-2q_0^2p^2+q_0^4/\zeta}}{2}}$ and $\delta(p) = \sqrt{\frac{-q_0^2+p^2+\sqrt{p^4-2q_0^2p^2+q_0^4/\zeta}}{2}}$.
After integration over θ, one finally gets

$$\begin{aligned}\frac{E_{int,P}(h)}{k_bTL^2} =& \frac{1}{2}\int_0^{\infty}\frac{pdp}{2\pi}\Big(\frac{F_1^2(p,h)}{F_1^2(p,0)} + \frac{\left(F_1(p,h)+p^2F_2(p,h)\right)^2}{\left(F_1(p,0)+q^2F_2(p,0)\right)^2} \\ &+\frac{\left(F_1(p,h)+F_4(p,h)\right)^2}{\left(F_1(p,0)+F_4(p,0)\right)^2} \\ &+\frac{2pF_3^2(p,h)}{(F_1(p,0)+p^2F_2(p,0))(F_1(p,0)+F_4(p,0))}\Big)\end{aligned}$$

The long-range behavior of this interaction energy is dominated by the term $\lim_{h\to\infty}\int_0^{\infty}\frac{pdp}{2\pi}\frac{(F_1(p,h)+F_4(p,h))^2}{(F_1(p,0)+F_4(p,0))^2} \propto \int_0^{\infty} dpp^2e^{-ph} \propto \frac{1}{h^4}$.

It is interesting to note that the long-range behavior in $1/h^4$ corresponds to the interaction between two thin dielectric plates[30]. The van der Waals interaction between thin metallic plates decreases in $1/h^2$. This situation is not well reproduced by the polarization freezing conditions. Molecular dynamics results mention that the molecules in the first layer of water in contact with metallic plates keep an important lability. The 2D rotation in the (x,y) plane is not constrained and water molecules exchange between first and second layer seems to be possible[33]. This dynamics can probably lead to non vanishing polarization fluctuations.

Appendix C: Sensitivity of characteristic lengths

In this Appendix, we calculate the sensitivity of the characteristic lengths that we determined in this paper as a function of the parameters q_0 and $\chi_{\parallel}^m$. We assume $\chi_{\parallel}^m = 40$ and $q_0 = 2.6$ $\mathring{A}^{-1}$.

In section II, we determined the ranges $r_{\parallel}^p$ and $r_{\perp}^p$ of the short-range longitudinal and transverse terms and the values ($f_{\parallel}^m$, $f_{\perp}^m$) and their position 2 $\lambda_{\parallel}$ of their maximum. The sensitivity of the given values for a small

change of q_0 or $\chi_\parallel^m$ are calculated as follow:

$$\begin{pmatrix} \frac{d2\lambda_\parallel}{2\lambda_\parallel} \\ \frac{df_\parallel^m}{f_\parallel^m} \\ \frac{df_\perp^m}{f_\perp^m} \\ \frac{dr_\parallel^p}{r_\parallel^p} \\ \frac{dr_\perp^p}{r_\perp^p} \end{pmatrix} = A \begin{pmatrix} \frac{dq_0}{q_0} \\ \frac{d\chi_m}{\chi^m} \end{pmatrix}$$

with the dimensionless matrix

$$A = \begin{pmatrix} \frac{q_0}{2\lambda_\parallel}\partial_{q_0} 2\lambda_\parallel & \frac{\chi_\parallel^m}{2\lambda_\parallel}\partial_\chi 2\lambda_\parallel \\ \frac{q_0}{f_\parallel^m}\partial_{q_0} f_\parallel^m & \frac{\chi_\parallel^m}{f_\parallel^m}\partial_\chi f_\parallel^m \\ \frac{q_0}{f_\perp^m}\partial_{q_0} f_\perp^m & \frac{\chi_\parallel^m}{f_\parallel^m}\partial_\chi f_\perp^m \\ \frac{q_0}{r_\parallel^p}\partial_{q_0} r_\parallel^p & \frac{\chi_\parallel^m}{r_\parallel^p}\partial_\chi r_\parallel^p \\ \frac{q_0}{r_\perp^p}\partial_{q_0} r_\perp^p & \frac{\chi_\parallel^m}{r_\perp^p}\partial_\chi r_\perp^p \end{pmatrix}.$$

The matrix A determined for $q_0 = 2.6\ \mathring{A}^{-1}$ and $\chi_\parallel^m = 40$ is equal to

$$A = \begin{pmatrix} -1.0 & 0.5 \\ 0 & 1.5 \\ 0 & 1.5 \\ -1.0 & 1.0 \\ -1.0 & 0.9 \end{pmatrix}$$

An increase, a decrease respectively, of $\chi_\parallel^m$, q_0 respectively, corresponds to an increase of the range of short-range terms. The sensitivity in q_0 and in $\chi_\parallel^m$ are similar for $r_{\parallel,\perp}^m$. The sensitivity is higher in q_0 for the position of the maximum $2\lambda_\parallel$. The value of the maximum $f_{\parallel,\perp}^m$ depends only on $\chi_\parallel^m$. For the set of parameters $(\chi_\parallel^m = 44, q_0 = 2.34)$, we obtain $(2\lambda_\parallel = 1.15 \quad \text{nm}, f_\parallel^m = 3.5, f_\perp^m = 3.9, r_\parallel = 3.1 \quad \text{nm}, r_\perp = 3.7 \quad \text{nm})$.

We also determine the sensitivity of λ_{point}, the decay length of hydrophobic interaction between two point-like particles. It is given by:

$$\frac{d\lambda_{point}}{\lambda_{point}} = \begin{pmatrix} \frac{q_0}{\lambda_{point}}\partial_{q0}\lambda_{point} & \frac{\chi_\parallel^m}{\lambda_{point}}\partial_\chi \lambda_{point} \end{pmatrix} \begin{pmatrix} \frac{dq_0}{q_0} \\ \frac{d\chi_\parallel^m}{\chi_\parallel^m} \end{pmatrix}$$

with $\begin{pmatrix} \frac{q_0}{\lambda_{point}}\partial_{q0}\lambda_{point} & \frac{\chi_\parallel^m}{\lambda_{point}}\partial_\chi \lambda_{point} \end{pmatrix} = (-0.5, 0.3)$. An increase, a decrease respectively, of $\chi_\parallel^m$, q_0 respectively, corresponds to an increase the decay length. The sensitivity is similar in both parameters. For the set of values $(\chi_\parallel^m = 44, q_0 = 2.34)$, we obtain λ_{point}=0.35 nm.

To finish, we determine the sensitivity of λ_{plate}, the decay of hydrophobic interaction between two plates. It is given by

$$\frac{d\lambda_{plate}}{\lambda_{plate}} = \begin{pmatrix} \frac{q_0}{\lambda_{plate}}\partial_{q0}\lambda_{plate} & \frac{\chi_\parallel^m}{\lambda_{plate}}\partial_\chi \lambda_{plate} \end{pmatrix} \begin{pmatrix} \frac{dq_0}{q_0} \\ \frac{d\chi_\parallel^m}{\chi_\parallel^m} \end{pmatrix}$$

with $\begin{pmatrix} \frac{q_0}{\lambda_{plate}}\partial_{q0}\lambda_{plate} & \frac{\chi_\parallel^m}{\lambda_{plate}}\partial_\chi \lambda_{plate} \end{pmatrix} = (-1.2, 1.4)$.

An increase, a decrease respectively, of $\chi_\parallel^m$, q_0 respectively, corresponds to an increase the decay length. The sensitivity is similar in both parameters. For the set of values $(\chi_\parallel^m = 44, q_0 = 2.34)$, we find λ_{plate}=0.21 nm.

[1] J. Israelachvili and R. Pashley, Nature **300**, 3412 (1982).
[2] M. U. Hammer, T. H. Anderson, and A. Chaimovich, Faraday Discuss. **103**, 15739 (2010).
[3] J. Das, C. Eun, S. Perkin, and M. L. Berkowitz, Langmuir **27**, 11737 (2011).
[4] G. Silbert, D. Ben-Yaakov, Y. Dror, S. Perkin, N. Kampf, and J. Klien, Phys. Rev. Lett. **109**, 168305 (2012).
[5] R. F. Tabor, C. Wu, F. Grieser, R. R. Dagastine, and D. Y. C. Chan, J. Phys. Chem . Lett. **4**, 3872 (2013).
[6] S. H. Donaldson, A. Royne, K. Kristiansen, M. V. Rapp, S. Das, M. A. Gebbie, D. W. Lee, P. Stock, M. Valtiner, and J. Israelashvili, Langmuir **6**, 1105911065 (2014).
[7] S. I. Mamatkulov, P. K. Khabibullaev, and R. R. Netz, Langmuir **20**, 4756 (2004).
[8] H. Li and M. Kardar, Phys. Rev. Lett. **67**, 3275 (1991).
[9] H. Li and M. Kardar, Phys. Rev. A. **46**, 6490 (1991).
[10] A. Ajdari, L. Peliti, and J. Prost, Phys. Rev. Lett. **66**, 1481 (1991).
[11] R. Golestanian, M. Goulian, and M. Kardar, Europhysics. Lett. **33**, 241 (1996).
[12] K. Lum, D. Chandler, and J. D. Weeks, J. Phys. Chem. B **103**, 4570 (1999).
[13] F. Sedlmeier, D. Horinek, and R. R. Netz, JACS **133**, 1391 (2011).
[14] D. Chandler, Nature **437**, 640 (2005).
[15] P. Varilly, A. J. Patel, and D. Chandler, J. Chem. Phys. **134**, 074109 (2011).
[16] E. H. Lieb, Phys. Rev. Lett. **18**, 692 (1967).
[17] P. Attard and M. T. Batchelor, Chem. Phys. Lett. **149**, 206 (1988).
[18] V. Korepin and P. Zinn-Justin, Journal of Physics A: Mathematical and General **33**, 7053 (2000).
[19] P. A. Bopp, A. A. Kornyshev, and G. Sutmann, Phys. Rev Lett. **76**, 1280 (1996).
[20] A. A. Kornyshev and G. Sutmann, Phys. Rev. Lett. **79**, 3435 (1997).
[21] P. A. Bopp, A. A. Kornyshev, and G. Sutmann, J. Chem. Phys. **109**, 1939 (1998).
[22] G. Jeanmairet, M. Levesque, R. Vuilleumier, and D. Borgis, J. Phys. Chem. Lett. **4**, 613 (2013).
[23] A. C. Maggs and R. Everaers, Phys. Rev. Lett. **96**, 230603 (2006).
[24] J. S. Pujos and A. C. Maggs, "Electrostatics of soft and disordered matter," (CRC Press, 2014) Chap. Legendre transforms for electrostatic energies.
[25] J. Mittal and G. Hummer, Proc. Natl. Acad. Sci. USA **105**, 20130 (2008).
[26] D. Bartolo, D. Long, and J.-B. Fournier, Europhys. Lett. **49**, 729 (2000).
[27] M. Kardar and R. Golestanian, Rev. Mod. Phys. **71**, 1233 (1999).
[28] R. C. Remsing, J. M. Rodgers, and J. D. Weeks, J Stat Phys **145**, 313 (2011).
[29] R. C. Remsing and J. D. Weeks, J. Phys. Chem. B **117**, 15479 (2013).
[30] J. Israelachvili, *Intermolecular & Surface Forces*, 2nd ed., edited by A. P. INC (Harcourt Brace & Company, Publishers, 1991).
[31] T. M. Raschke and M. Lavitt, Proc. Natl. Acad. Sci. U.S.A. **102**, 6777 (2005).
[32] N. Huang, D. Schlesinger, D. Nordlund, C. Huang, T. Tyliszczak, T. M. Weiss, Y. Acremann, L. G. M. Pettersson, and A. Nilsson, J. Chem. Phys. **136**, 074507 (2012).
[33] D. Laage, G. Stirnemann, and J. T. Hynes, J. Phys. Chem. B **113**, 2428 (2009).